Modeling Earth Systems and Environment (2020) 6:2047–2061
https://doi.org/10.1007/s40808-020-00772-3

ORIGINAL ARTICLE

An infrared thermography-based study on the variation in diurnal and seasonal land surface temperature at Dibrugarh city, India

Rituraj Neog[1] · Biman Lahkar[1] · Juri Baruah[1] · Shukla Acharjee[1] · Bijoy Shankar Gogoi[1] · Borakha Sonowal[1] · Dimpal Dutta[1] · Dimpee Chetia[1] · Jyotishma Baruah[1] · Madhusmita Gogoi[1] · Minakshi Patar[1] · Rajoshree Borah[1] · Tulika Das[1]

Received: 28 January 2020 / Accepted: 2 April 2020 / Published online: 30 July 2020

Abstract
The understanding of surface urban heat island pattern above Dibrugarh City has been studied through in situ observation using non-contact infrared thermometer for a period of 4 months by covering 16 selected locations. The chosen locations envelop both urban and suburban sites. The study draws attention to urban hot spots toward the central part of the city all through the different months in addition to the seasons, owing to heat retention supported by the built environment with fewer vegetation cover. Seasonally winter uncovered utmost variability of LST indicated by higher CV value. The core locations/sites witnessed a least amount of variability and continuity of higher LST throughout the learning months. At diurnal pattern, LST designated a sharp decrease from morning to afternoon period through winter months, while contrastingly summer months witnessed a sharp fall of LST from afternoon to night period. Among all the surfaces, asphalt pavement noticed maximum surface temperature with maximum variability in both diurnal and temporal scales. Maximum assimilation with fewer albedo of asphalt surface along with drier soil and grass comes across maximum LST in the internal part of the city. In addition, traffic, pollution and anthropogenic heat emission supported warmer surface temperature of asphalt, grass and bare soil, which on the whole put into the growth of higher surface heat. The stronger affirmative correlation coefficient amid the temperature of different surfaces with air temperature and comparatively weaker unconstructive correlation with relative humidity witnessed the dominant role of air temperature on overall surface urban heat island process.

Keywords LST · Diurnal scale · Variability · Surface temperature · Intensity

Introduction

Land surface temperature (LST) and its diurnal variation are crucial for the physical, chemical and biological processes of Earth. Climate-related studies were carried out to assess the environmental conditions and management practices on Earth surfaces, and their surrounding atmosphere requires LST information on a useful scale (Becker and Li 1993). Urbanization is a driver which brings a noticeable change in the natural surface of the Earth, and the natural surface is converted from bare soil or green area to the newly built surface (e.g., asphalt, stone, metal, concrete, etc.), thereby causing a change in the land cover. An urban heat island is a happening in which urban air temperature is comparatively higher than the adjoining rustic air temperature (Choi et al. 2014). Urban heat island intensity is mainly restricted by synthetic constructions in the urban environment as a consequence of extensive urbanization and industrialization (Oke 1973; Voogt and Oke 2003). Increased thermal capacity and relatively lower potentiality of evapotranspiration together with artificial temperature intensify the procedure of heat island intensity (Roth et al. 1989). Moreover, urban heat island consequences can as well be connected to climate strictures (Sundborg 1950; Chandler 1965; Unger et al. 2001). Further, skyscraping buildings and narrow roads reduce horizontal airflow (Liu and Zhang 2011). The unfavorable consequence of UHI is intense urban climate and thermal uneasiness (Almusaed 2011), rising utilization of power (Akbari and Konopacki 1998) and increasing per head water consumption, particularly during summer season (Guhathakurta and Gober 2007). It also leads to cool

✉ Rituraj Neog
rituraj.neog08@gamil.com

[1] Center for Studies in Geography, Dibrugarh University, Dibrugarh, India

demand in an urban locale during summer time of a year (Hu and Gensuo 2010). Heat island happening can be categorized into three types: boundary layer heat island, canopy layer heat island and surface urban heat island (Oke 1982). The first two develop over air, close to the urban surface to the crest of the building canopy, while the third one develops over the urban land surface (Voogt 2004). The surface urban heat island in general refers to the greater LST in an urban area than its rural equivalent (Yao et al. 2019). The land surface is a compound characteristic made up of impervious built-up, water body, open space and green areas. The LST is also identified as brightness as well as skin temperature, which can be determined by long wave radiation emanated from the land surface (Becker and Li 1995). The intensity of surface urban heat island intensity (SUHII) is based upon thermal conduct of surface materials and their revelation directly to the solar radiation (Sharifi and Soltani 2017). An urban area composed chiefly of solid construction with partial green areas and water bodies is accountable for the growth of intense LST and to finish with pilots to the SUHI process (Neog et al. 2019). The LST can be explored via different means such as satellite remote sensing as well as field measurement (Rasul et al. 2017). However, in recent times, field base readings over different surface materials by means of IR (infrared) thermometer has become a vital means to attend to the SUHII phenomenon (Kumar et al. 2017; Georgakis and Santamouris 2017; Neog et al. 2019). However, the spatiotemporal pattern of LST study by means of on-site observation with IR (infrared) thermometer with improved temporal resolution for a longer period of time is always deficient. Hence, an effort has been made to scrutinize the spatiotemporal pattern of land surface temperature, in order to address the subject of SUHII effect over Dibrugarh City and secondly to weigh up the function of different meteorological variables such as air temperature and relative humidity on thermal dynamicity of dissimilar surfaces.

Materials and methods

The study has been carried out over the urban areas of Dibrugarh over a period of 4 months. A total of 16 survey sites have been chosen covering town and uptown areas. The coordinates of the places are accessed using Garmin eTrex 30 GPS. The surface temperature data over 16 locations have been brought together using a non-contact IR thermometer. The LST data have been detected and documented from a distance of 60 cm over asphalt pavement (black top), bare soil (wet and dry) and grass. The emissivity value for respective surface materials has been attuned all through the compilation of data. The emissivity range for the IR thermometer varies from 0.1 to 1.0. The IR thermometer has a temperature resolution of 0.1 °C and a precision of ± 2 °C. The wavelength of the instrument ranges from 8 to 16 µm. The LST data are assembled for 12 days comprising 3 days for each month from February to May 2019. The campaign was started from February 21 to May 24, 2019. The months of February and March have been deemed for the winter spell, while April and May for the summer time of the year. To address the diurnal pattern, the study is splintered into three unique time slots, i.e., 11.00–11.30 am for the morning, 3.00–3.30 pm for the afternoon and 6.00–6.30 for the night. The mean LST of all locations (considering the different surfaces) is added with coordinates and as a final point, thermal zoning has been interpolated using the IDW method in QGIS 2.18.23. Furthermore, air temperature and relative humidity for the specified date and time have been collected by using a MicroLite data logger (self-recording) set with 1-min record interval. A total of 480 samples for air temperature and relative humidity are averaged to acquire the mean temperature and humidity condition during the learning stage. The data logger has a resolution of 0.01 °C for temperature and 0.2% for relative humidity. Similarly, it has an accuracy of 0.3 °C for temperature and 2% for relative humidity. The overall climate condition of Dibrugarh is evaluated form the online weather data, Dibrugarh https://www.timeanddate.com/weather/india/Dibrugarh. The simple ranking method has been employed for all the selected locations by handing over the first rank for the highest LST and consequently last ranks for the lowest LST for each month. And as a final point, a composite score/rank has been computed to put on view the whole LST pattern in the study areas. The land use land cover of the Dibrugarh municipal area has been prepared using Google Earth imagery for the year 2018. The KML file for all LULC layers has been extracted from Google Earth and converted into vector shape files in the GIS environment. The layers are reprojected into WGS 84 datum and UTM zone 46 North projections. The level I LULC classes are considered such as built-up, vegetation, agriculture, tea garden, water body and open areas/undeveloped areas. The areas of the respective LULC categories are anticipated from the attribute table of the vector layer. The municipal boundary map is collected from town and country planning organization (TCPO), Dibrugarh. The collected JPEG image is further georeferenced and projected using WGS 84 datum and UTM Zone 46 north projection. Further, ward frontier has been digitized using the projected municipal image. The municipal boundary has been used for the preparation of thermal map using the IDW (inverse distance weighted) interpolation technique. The rose diagram has been prepared using GeoRose software to display the average speed and direction of the wind during the study days. The detailed methodology is represented in Fig. 1.

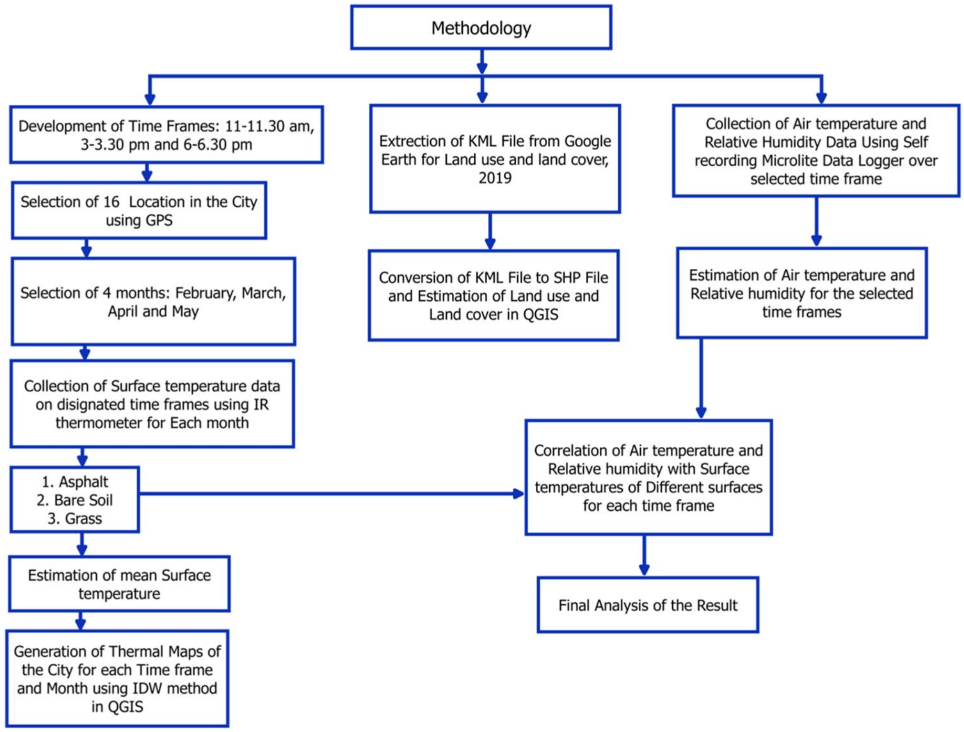

Fig. 1 Flowchart of methodology

Study area

Dibrugarh City is located in the south bank of river Brahmaputra in upper Assam. The city is considered as the third largest urban agglomeration of Assam in terms of population size. It is the administrative headquarter of the Dibrugarh District of Assam. The total municipal area of Dibrugarh City is 15.60 km^2. It has a total urban population of 1, 38,661 (Census of India 2011) distributed over 22 municipal wards. The coordinates of the urban centre are 94° 54′ E longitude and 27° 28′ N latitude. The city is located in the relatively flat alluvial plain with a mean elevation of 104 m above mean sea level. The city is below subtropical monsoonal climate with minimum and maximum temperature of winter and summer ranging from 11 to 32 °C (https://www.timeanddate.com/weather/india/dibrugarh/climate). As per the classification of Koppen, the city of Dibrugarh falls under the CWG climate. Dibrugarh City symbolizes a populace compactness of about 8945 persons/km^2. The population of Dibrugarh town is spread over 22 municipal wards with a maximum population density in core urban wards of 9, 10, 13, 17, 19 and 20, respectively. Dibrugarh City takes up a major part of the land as the built-up area with 41.11% followed by the next dominating land cover categories such as open space (35.87%), vegetation (16.14%), tea garden (5.45%), water body (0.76%) and paddy field (0.74%). The spatial pattern of land use and land cover of Dibrugarh City is represented in Fig. 2.

Results and discussion

Climatic condition of the study area

The study area is under a monsoonal tropical climate. The mean temperature of Dibrugarh City during the study period ranges from 24.94 to 35.84 °C (based on the data collected by MicroLite data logger). While relative humidity varies from 41.85 to 73.26%, minimum air temperature has been recorded during February, whereas the maximum during the month of April. Wind speed and the direction along with air pressure have been estimated using the data provided by Mohanbari Meteorological Station, Dibrugarh. Figure 3 clearly illustrates the dominant wind direction as NE (north–east) with an average wind of 8.7 km per hour. However, maximum recorded wind speed has been observed from NNE (north–northeast) direction with a mean wind speed of 13 km per hour.

Seasonality of LST

The study assessed the seasonal land surface temperature (LST) for the city. As depicted in Figs. 4 and 5, relatively higher LST has been observed in the core urban areas, while lower in the peripheral parts of the city. Seasonally, overall summer time LST is more than winter (Fig. 6). However, the intensity of LST (range between maximum and minimum) is computed as more in winter than summer, i.e., 5.31 °C and 4.72 °C, respectively. This might be due to relatively lower

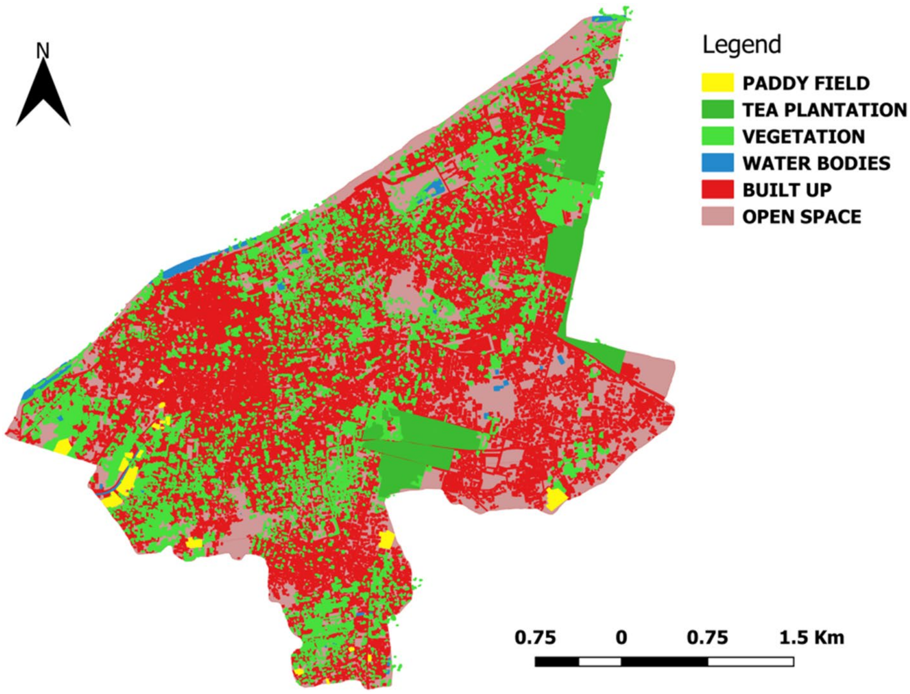

Fig. 2 Land use land cover, Dibrugarh, 2019

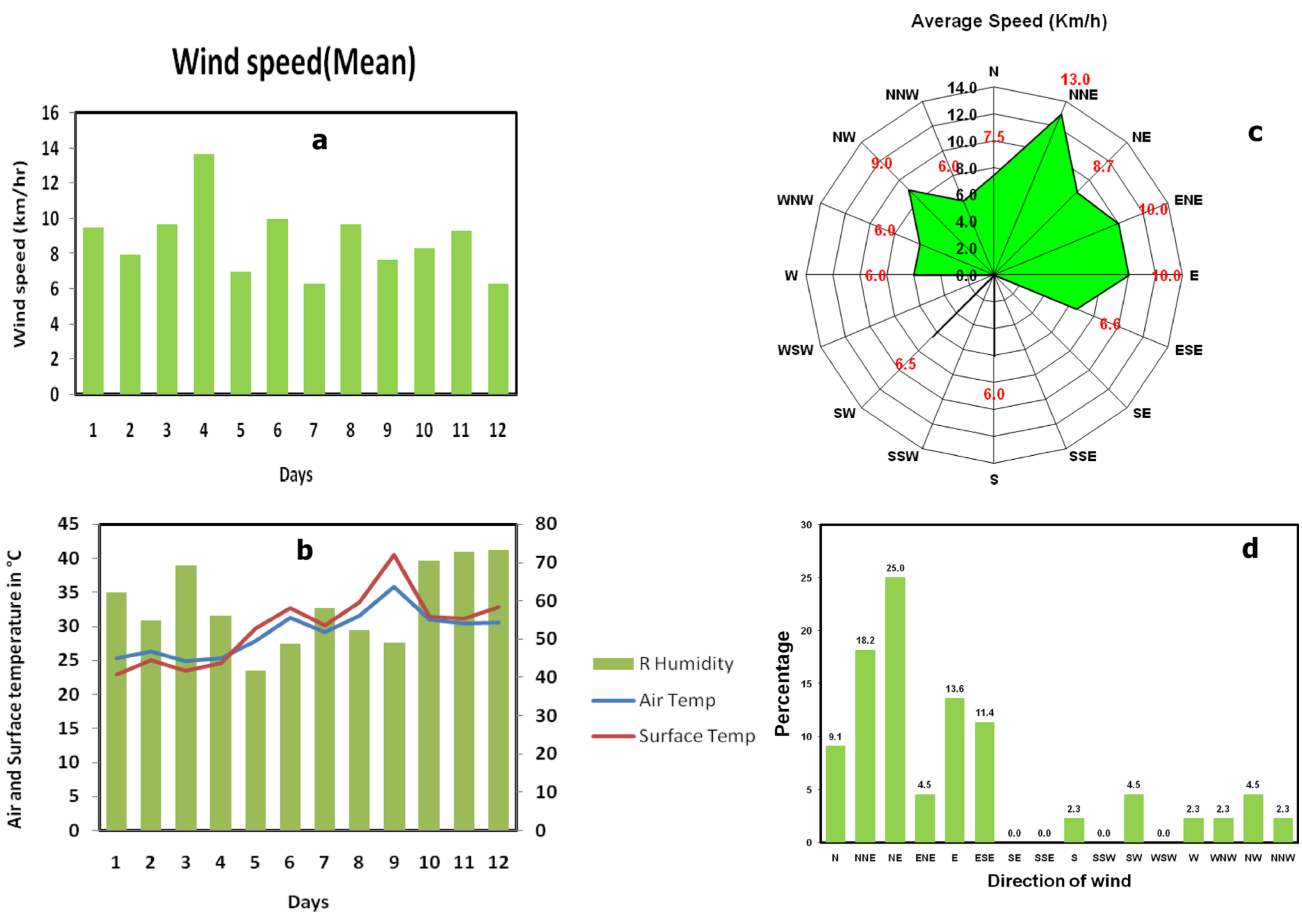

Fig. 3 Atmospheric condition of study area during the selected days (**a** bar graph showing mean wind speed, **b** trend of relative humidity, air temperature and surface temperature, **c** mean wind speed and direction, **d** distributional pattern of wind direction)

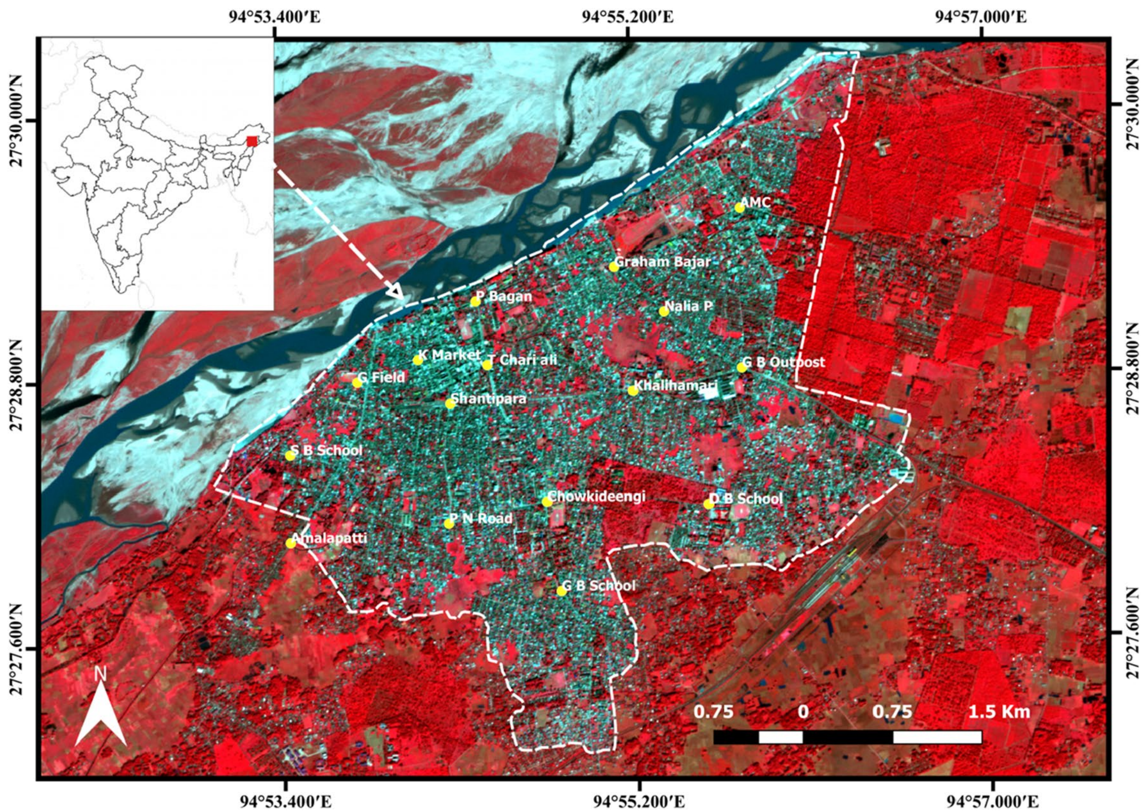

Fig. 4 Location of the study sites, Dibrugarh City, 2019

LST in the peripheral parts of the city as an outcome of a lower built environment, less vegetation cover with wind effect and rapid cooling by nocturnal radiation and contrastingly upholding of LST in urban counterpart. The mean LST of winter is 26.47 °C, while that of summer is 33.28 °C. Thus, overall 6.81 °C rise of LST is detected between the selected seasons. The SD value of 1.57 and 1.33 for winter and summer witnessed lower variability of LST in the summer season. Spatially as depicted in the interpolated map (Fig. 5), higher surface temperature or urban hot spots are dominated toward the north central part of the city during February and its dispersal as well as maximum development over March and April and lastly a southerly budge during the month of May (Fig. 5).

Monthly pattern of LST

The mean LST of the months has given away a quite different pattern by revealing a intensifying tendency of LST, i.e., 23.91 °C, 29.02 °C and 34.76 °C from the month of February to April with slight retreating of LST to 31.79 °C in the month of May. The falling pattern of LST in the month of May is the outcome of cloud cover with increasing relative humidity and decreasing air temperature. As mentioned in Tables 1 and 2, the locations 5, 6, 9, 10, 11 and 12 depicted maximum LST all throughout the study period, while the locations 4, 13, 14 and 15 depicted minimum LST. Uncommonly, less LST specifically in the location 4 (urban) might be developed by daytime shade provided by buildings. The development of maximum LST in aforesaid location is the result of the urban area with dense built-up, traffic, pollution with less vegetal cover, while the minimum at suburban sites is proscribed by relatively less built-up area with adequate greeneries. The maximum intensity of LST of 5.95 °C is observed during the month of March followed by May, February and April. Interestingly, SD value also revealed mostly similar order with the maximum in the month of March followed by May, April and February. However, CV portrays maximum during winter months, while minimum during summer months. The maximum variability of LST during winter months might be the results of heat retention in urban part developed by the built environment, human activities, pollution and traffic, while relatively lacks such effect in the suburban areas along with the rapid cooling effect resulted during the winter season. The urban locations such as 9, 10, 11 and 12 address overall minimum CV during the study month, which indicated again the continuity of LST or minimum variation of LST in the core urban areas. Additionally,

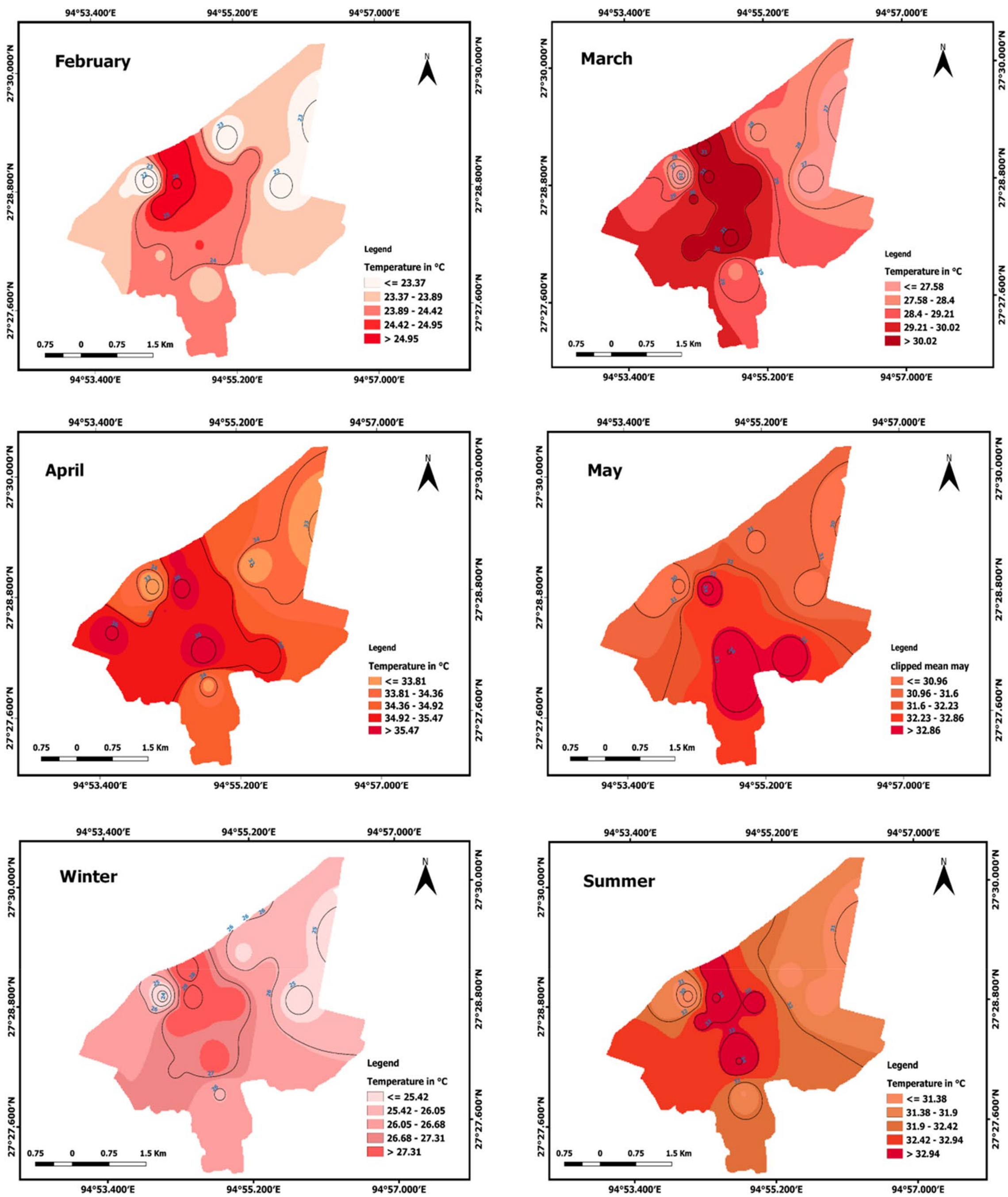

Fig. 5 Pattern of LST over Dibrugarh City during February to May along with seasonal contrast, 2019

cooling and shading effects of green areas in the suburban as well as in the peripheral part of the city also play a central role in lower or quick diminution of LST, mostly during the winter season, which becomes useful in developing the maximum variability pattern of LST between urban and suburban areas. The variability pattern of LST during different months is illustrated in Fig. 5.

Diurnal pattern of LST

LSTs showed significant variations during the daytime and nighttime in the city. The overall rate of reduction in LST among the selected time frame has been anticipated for every month. The outcome reveals a sharp decrease in the rate of LST during the morning to afternoon phase from

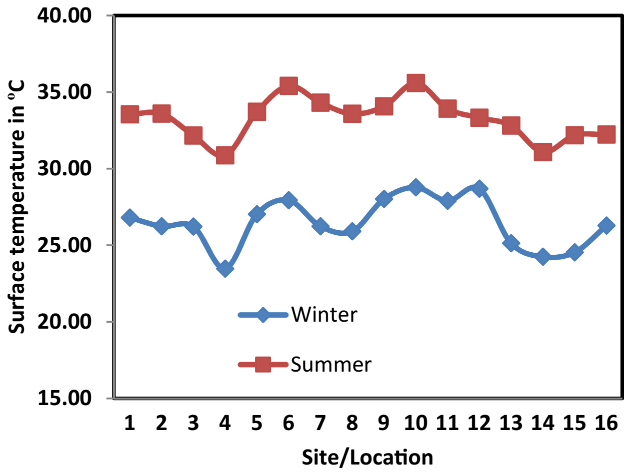

Fig. 6 Seasonal pattern of surface temperature over different locations, Dibrugarh, 2019

February to March, while the slower pace of decrease in LST was depicted during the later months such as April and May, but on the other hand, the mounting rate of LST reduction from afternoon to night phase was depicted during the later months. This might be mainly due to less duration and intensity of sunbeams during the winter period which caused a sharp fall of surface temperature mostly in the suburban sites/location during the morning to afternoon period, while the rate of decline of LST during the afternoon to night showed somewhat a different temperament. It was observed as minimum during February, while maximum toward the later months with the utmost in the April month. This might be owing to dry weather and extreme insolation mostly during March and April, causing peak LST during daytime and sharp decline at night. The SD value points out the minimum variability of LST among different time frames (among all the sites) during February and its uphill trend in the ensuing months. The CV signifies maximum variability of LST in the daybreak period mostly during February and March and a declining rate toward the later months. Similarly, afternoon also represented a comparable pattern with maximum variability of LST in the previous months. CV depicted to a certain extent an odd pattern at night phase showing its maximum in March and May while less significant during February and April. Similarly on the whole intensity of LST (considering maximum and minimum among all sites constituting selected time frames) has shown ascending rate for the rest of the months excluding April. However, the sliding rate of CV is computed from winter to summer time of year with the highest during March. During the morning time, the maximum intensity of LST is noticed for March (10.47 °C) followed by February (7.75 °C), April (6.51 °C) and May (5.27 °C). While the afternoon phase put on view dissimilar pattern with maximum intensity in March (7.89 °C) followed by May (7.11 °C), April (6.58 °C) and February (6.05 °C), the maximum intensity of LST for night is computed for May (6.62 °C), followed by March (6.38 °C), April (4.3 °C) and February (3.50 °C). The spatial pattern of LST development during different times of the day as well as month is represented in Fig. 7.

Temporal pattern of LST over different surfaces

A study was carried out over three surfaces: asphalt road, grass and bare soil, to find out the temporal pattern of LST over these surfaces. The study witnessed a notable variability pattern of surface temperature among different land surfaces at the diurnal, monthly and seasonal scales. By and large asphalt road surface noticed the highest mean surface temperature of 35.64 °C, whereas grass and bare soil noticed 29.50 °C and 30.25 °C, respectively. Alike at every setting asphalt surface turns out to be hotter than bare soil and grass (Table 3). Thus, asphalt happens to be the hottest, while bare soil is warmer than grass (Yilmaz et al. 2008). Likewise, asphalt surface depicted utmost variability of surface temperature, than grass and bare soil (considering the mean of all the selected time frame), i.e., 9.73 °C, 4.45 °C and 3.67 °C, respectively. While looking into the diurnal scale, variation of the surface temperature of asphalts roadway from grass and bare soil is rather higher at daylight than at the night, at diurnal scale, maximum variability (based on range) of an asphalt surface is examined during the daytime, while the least at hours of darkness. On the other hand, grass cover flaunted maximum variability at nighttime while minimum during the daytime. But surprisingly, bare soil symbolizes sequential increment of the variability of surface temperature from crack of dawn to nighttime. At spatial scale, asphalt surface once more depicted maximum variability than grass and bare soil. The mean variation of surface temperature of asphalt and bare soil is 5.38 °C, which is a little lesser than the mean difference of asphalt and grass, i.e., 6.14 °C, while the mean dissimilarity of surface temperature of grass and bare soil is only 0.75 °C (Table 4). Yilmaz et al. (2008) identified the mean difference of surface temperature between asphalt and grass, asphalt and soil and soil and grass as 11.79 °C, 6.5 °C and 5.3 °C, respectively. In general, at all the diurnal scale (11.30 am, 3.30 pm and 6.30 pm), the mean difference of surface temperature between asphalt and grass is the highest, while that of bare soil and grass is the lowest. Even though the supreme dissimilarity between the abovementioned two of a kind surface temperature at the chosen time niche becomes more noticeable in the day period, the variability pattern of asphalt, bare soil and grass during different diurnal phases is depicted in Fig. 8 and Table 4.

Table 1 Diurnal and monthly pattern of LST over different location, Dibrugarh, 2019

Sites/locations	February (surface temp in °C)				March (surface temp in °C)				April (surface temp in °C)				May (surface temp in °C)			
	11–11.30 am	3–3.30 pm	6–6.30 pm	Mean	11–11.30 am	3–3.30 pm	6–6.30 pm	Mean	11–11.30 am	3–3.30 pm	6–6.30 pm	Mean	11–11.30 pm	3–3.30 pm	6–6.30 pm	Mean
1	26.36	24.86	19.65	23.62	39.66	28.93	21.41	30.00	42.74	36.28	26.79	35.27	36.13	33.42	25.90	31.82
2	28.84	22.64	18.91	23.46	36.92	28.52	21.63	29.02	42.35	39.94	26.19	36.16	34.12	33.66	25.33	31.04
3	27.08	23.86	19.02	23.32	36.27	30.04	21.07	29.13	39.37	36.27	26.99	34.21	32.16	32.49	25.71	30.12
4	24.66	21.77	17.94	21.46	31.26	25.72	19.48	25.49	37.23	34.42	25.26	32.30	31.62	31.36	25.34	29.44
5	26.87	24.54	20.18	23.86	35.98	31.28	23.37	30.21	39.62	37.49	29.10	35.41	32.36	33.37	30.34	32.02
6	28.24	24.96	20.14	24.44	37.00	33.62	23.70	31.44	43.28	38.32	28.77	36.79	34.96	35.52	31.61	34.03
7	28.35	23.93	18.63	23.64	34.16	30.89	21.51	28.85	41.69	36.75	26.95	35.13	35.51	34.63	30.32	33.49
8	26.98	24.24	19.93	23.72	34.07	27.74	22.53	28.11	39.34	34.73	26.86	33.65	35.12	35.54	29.90	33.52
9	30.06	27.03	20.72	25.94	33.66	33.48	23.19	30.11	37.71	40.43	28.29	35.48	34.94	35.79	27.26	32.66
10	29.90	27.82	20.97	26.23	35.64	33.44	24.92	31.34	39.13	41.01	29.56	36.57	36.90	37.94	29.02	34.62
11	29.57	24.76	20.22	24.85	37.41	31.16	24.33	30.97	39.61	37.67	28.52	35.26	33.76	35.76	28.19	32.57
12	32.42	24.27	21.21	25.96	40.64	29.80	23.86	31.43	42.71	36.47	27.71	35.63	33.84	32.09	27.12	31.02
13	26.22	22.64	18.66	22.51	33.41	29.43	20.45	27.76	39.51	37.32	27.86	34.89	32.66	33.62	25.93	30.74
14	28.04	22.13	17.70	22.62	32.91	26.21	18.54	25.89	36.76	35.18	25.61	32.52	32.45	30.83	25.65	29.64
15	26.60	23.30	18.28	22.73	30.16	28.49	20.39	26.35	39.18	36.61	25.71	33.83	33.97	32.61	24.99	30.52
16	27.86	25.52	19.44	24.27	34.98	29.71	20.21	28.30	37.11	35.83	26.02	32.99	35.14	33.77	25.51	31.47
Mean	28.00	24.27	19.47	23.91	35.26	29.90	21.91	29.02	39.83	37.17	27.26	34.76	34.10	33.90	27.38	31.79
S.D	1.88	1.64	1.08	1.34	2.79	2.37	1.86	1.95	2.13	1.94	1.33	1.37	1.54	1.87	2.20	1.58
C.V	6.70	6.76	5.53	5.59	7.91	7.94	8.49	6.70	5.35	5.22	4.88	3.95	4.51	5.53	8.04	4.95
Max	32.42	27.82	21.21	26.23	40.64	33.62	24.92	31.44	43.28	41.01	29.56	36.79	36.90	37.94	31.61	34.62
Min	24.66	21.77	17.70	21.46	30.16	25.72	18.54	25.49	36.76	34.42	25.26	32.30	31.62	30.83	24.99	29.44
Range	7.75	6.05	3.51	4.78	10.48	7.89	6.38	5.95	6.52	6.59	4.30	4.49	5.28	7.11	6.62	5.18

Table 2 Spatial pattern of surface temperature over different month, Dibrugarh, 2019

Site	Name	Location	Surface temperature in °C				Ranking				
			February	March	April	May	R^1	R^2	R^3	R^4	CR
1	J G Path	Sub-urban	23.62	30.00	35.27	31.82	10	7	7	8	32
2	Amolapatty	Sub-urban	23.46	29.02	36.16	31.04	11	9	3	10	33
3	G S Road	Sub-urban	23.32	29.13	34.21	30.12	12	8	11	14	45
4	Cole road	Urban	21.46	25.49	32.30	29.44	16	16	16	16	64
5	PN road	Urban	23.86	30.21	35.41	32.02	7	5	6	7	25
6	C Chari ali	Urban	24.44	31.44	36.79	34.03	5	1	1	2	9
7	Don Bosco Tiniali	Sub-urban	23.64	28.85	35.13	33.49	9	10	9	4	32
8	Mankota Road	Urban	23.72	28.11	33.65	33.52	8	12	13	3	36
9	Santipara	Urban	25.94	30.11	35.48	32.66	3	6	5	5	19
10	T Chari Ali	Urban	26.23	31.34	36.57	34.62	1	3	2	1	7
11	Khalihamari	Urban	24.85	30.97	35.26	32.57	4	4	8	6	22
12	PhulBagan	Urban	25.96	31.43	35.63	31.02	2	2	4	11	19
13	AMC Road	Urban	22.51	27.76	34.89	30.74	15	13	10	12	50
14	AMC Gate	Sub-urban	22.62	25.89	32.52	29.64	14	15	15	15	59
15	G P Outpost	Sub-urban	22.73	26.35	33.83	30.52	13	14	12	13	52
16	Naliapool	Sub-urban	24.27	28.30	32.99	31.47	6	11	14	9	40

Relationship pattern of LST with Air temperature and Relative humidity

The rapport flanked by the surface temperature of unlike surfaces such as asphalt, grass and bare soil is correlated with atmospheric parameters, i.e., air temperature and relative humidity. In isolation, surface temperature of asphalt, grass and bare soil calculated a very strong sanguine relationship with air temperature with an R value of 0.979, 0.984 and 0.981 along with r^2 of 0.959, 0.970 and 0.963, respectively. The aforementioned relationships are accepted as noteworthy supported by a p value of 0.0001 with a 5% level of significance. In contrast, feeble negative correlation coefficient is addressed for the surface temperature of asphalt, grass and bare soil with relative humidity with an R value of -0.222, -0.181, -0.262 and r^2 of 0.04, 0.03 and 0.06 correspondingly. Even if the affiliation is accepted as insignificant with a 5% level of significance, on the whole high positive as well as significant correlation coefficient is acknowledged for air temperature and surface temperature during 11.30 am, 3.30 pm and 6.30 pm with an R value of 0.904, 0.977 and 0.965 in the same way. But captivatingly the liaison becomes pretty stronger in the afternoon as well as at nighttime. Likewise, for the aforesaid relationship calculated r^2 values are 0.817, 0.955 and 0.932, respectively. Contrastingly, surface temperature behaves in a different way with relative humidity by developing a moderate negative correlation coefficient during 11.30 am and relatively weak negative relationship at 3.30 pm, but unexpectedly weak constructive relationship was witnessed at 6.30 pm which is supported by an R value of -0.541, -0.165 and 0.103, respectively.

At the diurnal scale, different surfaces such as asphalt, grass and bare soil gave a picture of dissimilar pattern with respect to air temperature and relative humidity. The surface temperature of asphalt introduced ascending strength of positive correlation coefficient with air temperature by an R value of 0.91, 0.94 and 0.97, but interestingly sliding negative correlation coefficient with relative humidity is supported by an R value of -0.44, -0.11 and -0.01 at 11.30 am, 3.30 pm and 6.30 pm, respectively. Nearly a comparable pattern of correlation is also observed among the surface temperature of uncovered soil and air temperature for the above-mentioned time frame with an R value of 0.90, 0.96 and 0.94 and conversely negative weak correlation coefficient with relative humidity again with an R value of -0.49 and -0.23 at 11.30 am and 3.30 pm, while weak positive correlation with an R value of 0.13 for 6.30 pm. Grass as well analyzed quite a strong positive relationship with air temperature, i.e., 0.89. 0.72 and 0.92, but most interestingly relatively negative correlation happens to be subjugated only during the daybreak period (11.30 am) with a calculated R value of -0.48 and weak positive correlation witnessed during the ensuing time frame with an R value of 0.13 and 0.20, respectively. As a result, in general, air temperature has strong and considerable impact over the development of surface temperature, particularly at night, while the influence of relative humidity over surface temperature is established as faintly influencing but inconsequential during sunup period (11.30) and chronologically

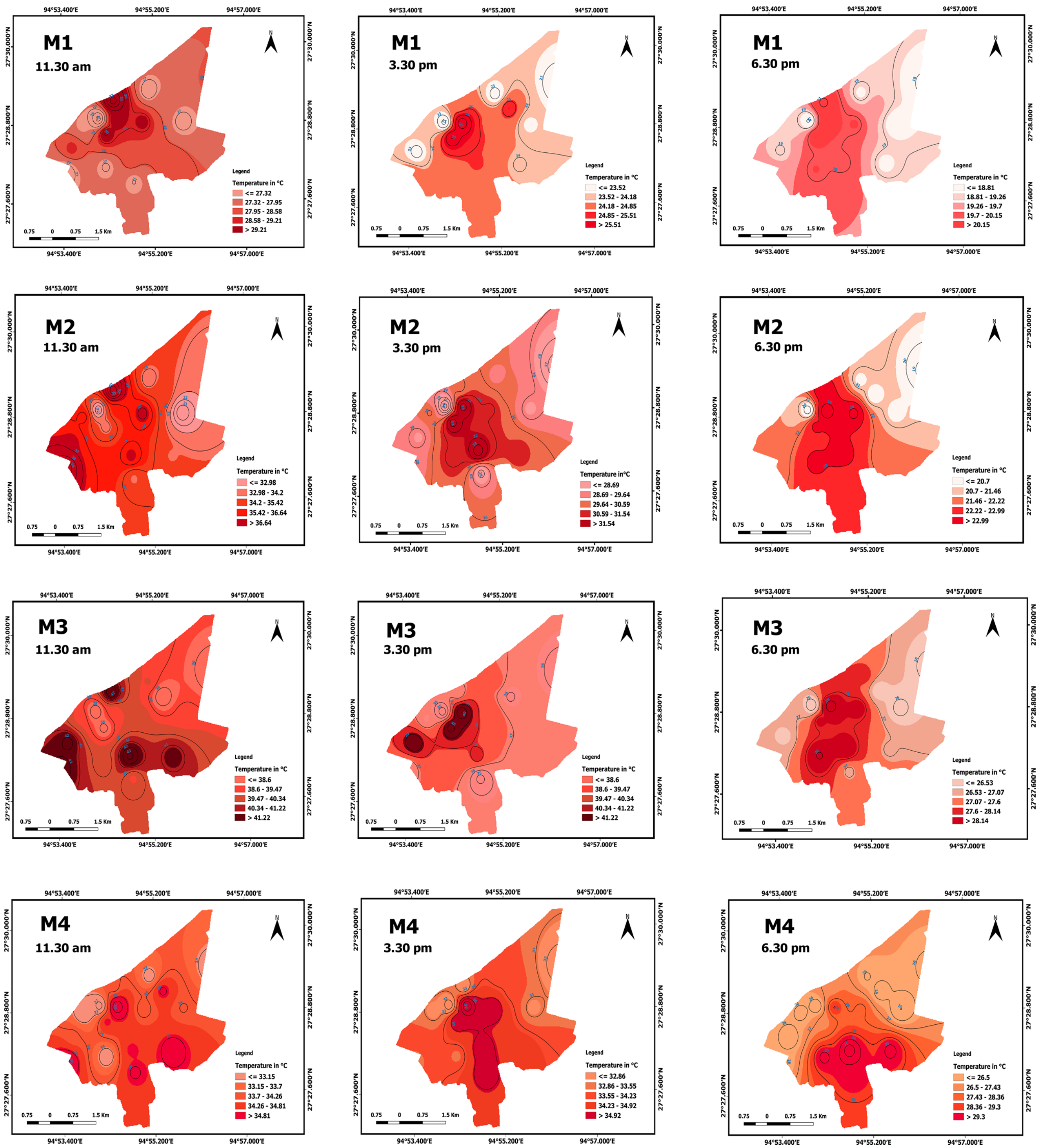

Fig. 7 Spatial and diurnal pattern of land surface temperature: M1, February, M2, March, M3, April, M4, May, Dibrugarh, 2019 (interpolated using inverse distance weighted method)

weaker toward the rest of the time frame (i.e., during the afternoon and night). In the same way, wind speeds also symbolize a negative correlation coefficient with air temperature and surface temperature with R and r^2 of -0.36 and -0.40 and 0.16 and 0.13, respectively (Fig. 9). As mentioned in Table 5, air temperature has a noteworthy correlation with surface temperature of different substances, while an insignificant relationship with relative humidity at the chosen time frame.

Table 3 Mean Surface temperature of Asphalt, Bare soil and Grass, Dibrugarh, 2019

Locations	Surface temperature (in °C)		
	Asphalt	Bare Soil	Grass
1	35.51	30.14	29.81
2	35.77	28.39	28.95
3	33.39	29.28	27.68
4	32.38	28.42	27.52
5	36.41	30.77	28.89
6	38.08	32.03	31.98
7	37.23	32.01	31.22
8	37.31	31.94	31.32
9	35.74	31.91	30.34
10	41.11	32.07	30.68
11	37.16	30.42	30.14
12	34.87	29.43	28.76
13	33.32	29.28	29.62
14	31.37	29.48	28.07
15	34.82	28.96	27.79
16	35.73	29.49	29.19

Discussion

The urbanized area surfaces mainly comprise built-up land and anthropogenic material, whereas the peripheral areas comprise agricultural fields, barren soil and forest. Thus, one of the primary reasons behind the difference in SUHII pattern may be the material property. In general, the study highlighted the development of LST mostly in the central part of the city dominated by the built environment with petite or no plant life (Fig. 2). The seasonally utmost intensity of LST in winter is caused by less insolation along with the rapid diminution of surface temperature in the peripheral part of the city supported by open space and vegetation. The core urban settings retain overall minimum seasonal and monthly variations of surface temperature developed due to the concentration of maximum urbanized quarters with traffic jamming and pollution. The maximum surface temperature during the month of April is the outcome of a dry milieu, low wind speed and uprising intensity of insolation. Although the comparatively slight withdrawing pattern of surface temperature through the month of May is the effect of cloud cover and wind, there is at all times an inverse relationship between cloud cover and surface temperature (Shamsipour et al. 2013). As a general rule, utmost surface temperature of asphalt is connected to maximum absorption of sunbeams, while on the other hand, minimum in grass is caused by higher reflection. Similarly, maximum variability pattern of surface temperature of asphalt might be due to differences resulted from traffic movement, pollution, wind and shadowing effect of vegetation. More often than not, dynamicity of surface temperature of asphalt surface resulted in net variability in the surface

Table 4 Mean difference of Surface temperature between Asphalt, Bare soil and Grass at different diurnal scale, Dibrugarh, 2019

Location	Mean Difference of Surface Temperature in °C (11.30–12.00 am)			Mean Difference of Surface Temperature (03.30–04.00 pm) in °C			Mean Difference of Surface Temperature (06.30–07.00 pm) in °C		
	Asphalt and bare soil	Asphalt and grass	Bare soil and grass	Asphalt and bare soil	Asphalt and grass	Bare soil and grass	Asphalt and bare soil	Asphalt and grass	Bare soil and grass
1	4.20	4.80	0.60	7.17	7.87	0.70	4.72	4.43	−0.28
2	8.42	5.88	−2.53	9.52	10.25	0.73	4.18	4.32	0.13
3	3.68	6.35	2.67	5.05	6.78	1.73	3.58	4.00	0.42
4	3.55	5.28	1.73	5.58	6.00	0.42	2.73	3.28	0.55
5	7.30	10.18	2.88	5.77	7.63	1.87	3.85	4.73	0.88
6	5.90	7.28	1.38	8.00	7.85	−0.15	4.25	3.17	−1.08
7	5.03	6.03	1.00	6.75	6.37	−0.38	3.88	5.65	1.77
8	6.85	6.83	−0.02	5.92	6.85	0.93	3.32	4.28	0.97
9	2.90	5.53	2.63	6.10	7.78	1.68	2.50	2.87	0.37
10	11.30	13.35	2.05	10.60	12.03	1.43	5.23	5.90	0.67
11	6.60	6.87	0.27	8.53	9.10	0.57	5.08	5.08	0.00
12	7.30	7.58	0.28	6.83	8.38	1.55	2.20	2.38	0.18
13	3.47	2.90	−0.57	5.53	4.85	−0.68	3.12	3.33	0.22
14	1.62	3.13	1.52	2.32	3.00	0.68	1.73	3.77	2.03
15	6.62	6.87	0.25	7.60	9.83	2.23	3.35	4.38	1.03
16	6.93	4.98	−1.95	8.63	11.17	2.53	3.13	3.45	0.32
Mean	5.73	6.49	0.76	6.87	7.86	0.99	3.55	4.06	0.51

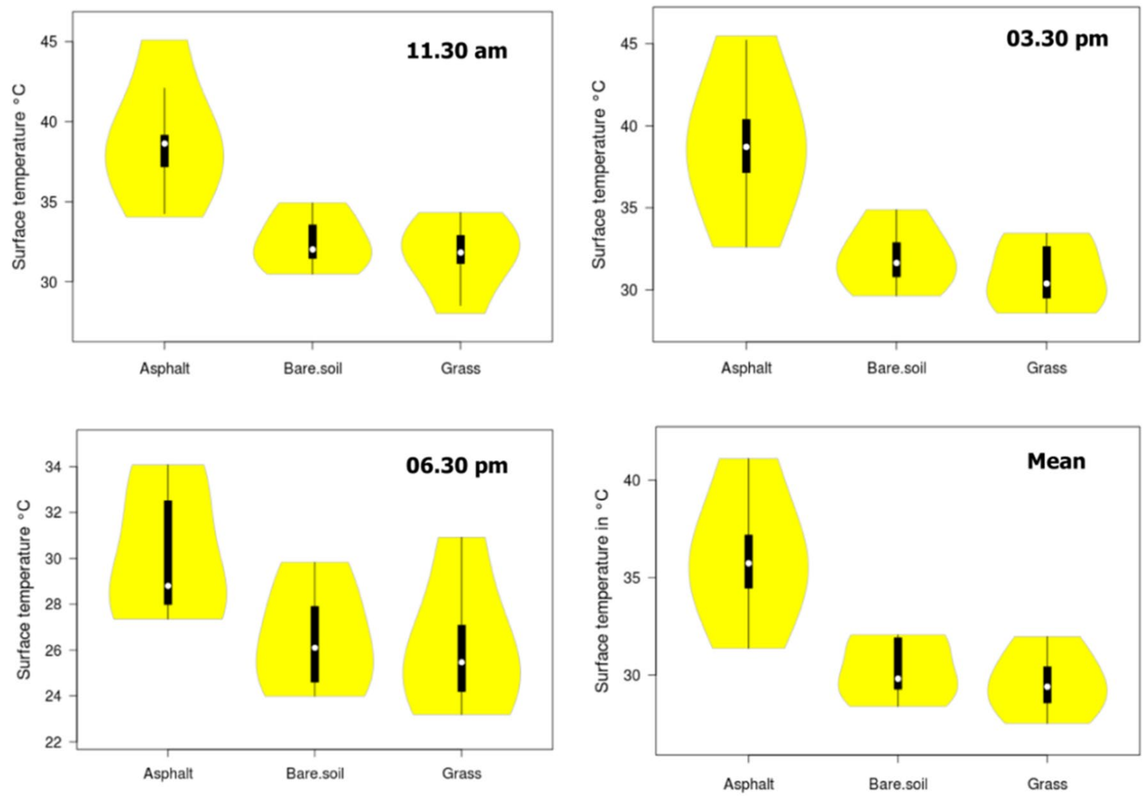

Fig. 8 Violin plots showing diurnal variability of surface temperature of asphalt, bare soil and grass, Dibrugarh, 2019

temperature pattern of the entire municipality. Perhaps, maximum traffic and pollution together with heat trap has resulted in higher asphalts land surface temperature mostly in the interior part of the city. Correspondingly, the existence of relatively dry soil and grass toward the inner part of the city contributes somewhat higher surface temperature, which turns out to be supportive for maximum LST in the central part of the urban locations. The overall high upbeat liaison between air temperature and surface temperature of asphalt, soil and grass witnessed ascendancy of air temperature for the diurnal, monthly and seasonal dynamics of the surface temperature pattern of the city. However, the influence of relative humidity is fairly narrow over surface temperature patterns. As cited in the preceding segment, wind speed is also liable for the slight change in temperature pattern of both surfaces and air, while negligible over relative humidity pattern. Thus, by and large higher air temperature with low wind speed and humidity joined with built-up area, traffic and pollution on the whole can shore up the development course of surface urban heat island intensity.

Fig. 9 Scatter plot showing relationship between surface temperature ▶ and atmospheric parameters (air temperature and relative humidity), **a** asphalt and air temperature, **b** bare soil and air temperature, **c** grass and air temperature, **d** asphalt and relative humidity, **e** bare soil and relative humidity, **f** grass and relative humidity, relationship between surface and air temperature (**a1** 11.30 am, **b1** 3.30 pm, **c1** 6.30 pm), relationship between surface temperature and relative humidity (**e1** 11.30 am, **f1** 3.30 pm, **g1** 6.30 pm), **d1** mean surface temperature and air temperature, **h1**- mean surface temperature and relative humidity

Conclusion

The study highlighted the expansion of surface heat island phenomena and its spatiotemporal dynamics over Dibrugarh City. By and large, core urban area with the built environment and soaring populace concentration develops urban hot spots. The intensity of surface temperature becomes further noticeable with maximum variability in the winter season. Concrete and asphalt materials are the common materials usually found in the urban areas as they are used for most surface construction. These materials mostly absorb and store heat energy much more effectively

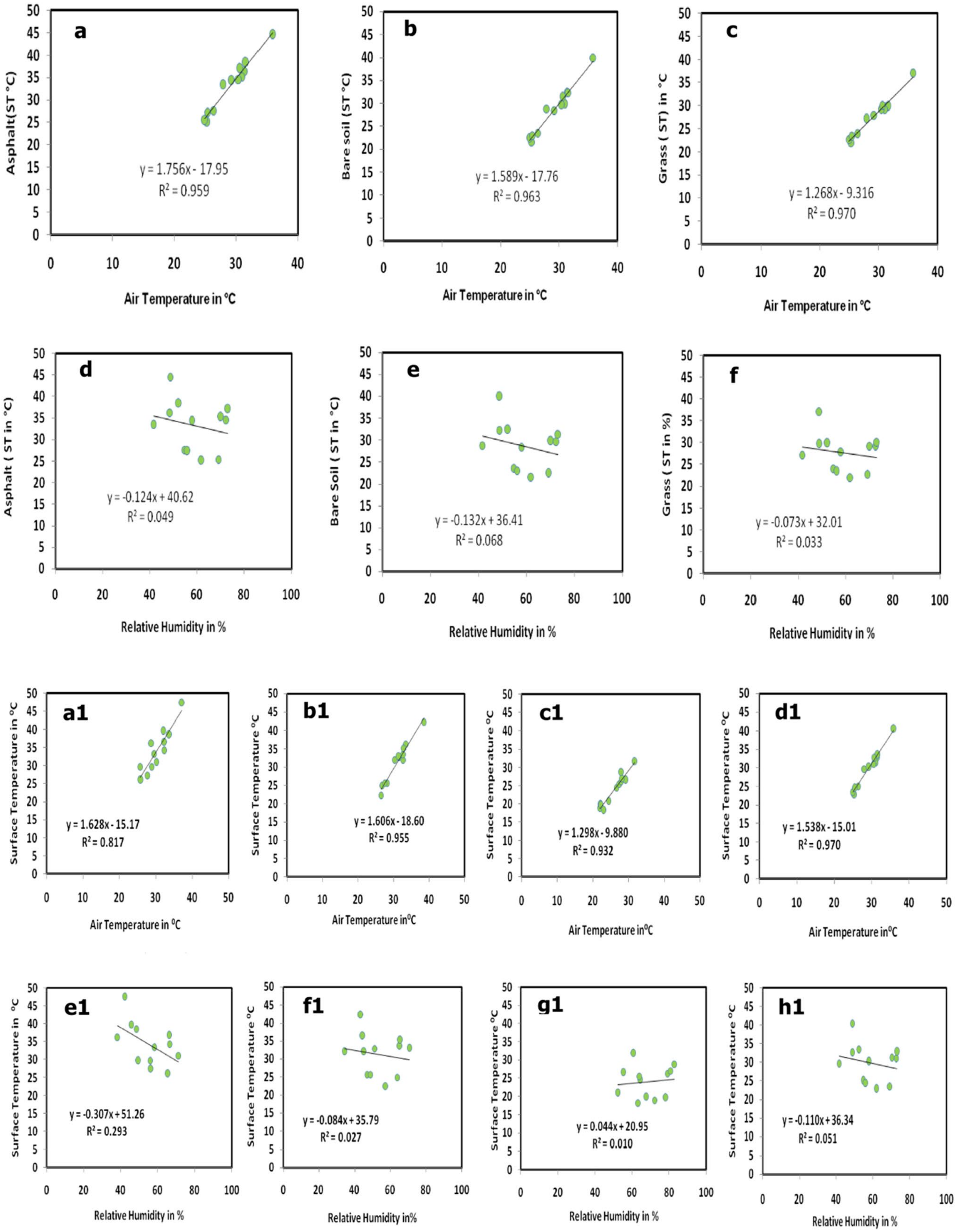
a
Asphalt(ST °C)
y = 1.756x - 17.95
R² = 0.959
Air Temperature in °C
b
Bare soil (ST °C)
y = 1.589x - 17.76
R² = 0.963
Air Temperature in °C
c
Grass (ST) in °C
y = 1.268x - 9.316
R² = 0.970
Air Temperature in °C
d
Asphalt (ST in °C)
y = -0.124x + 40.62
R² = 0.049
Relative Humidity in %
e
Bare Soil (ST in °C)
y = -0.132x + 36.41
R² = 0.068
Relative Humidity in %
f
Grass (ST in %)
y = -0.073x + 32.01
R² = 0.033
Relative Humidity in %
a1
Surface Temperature in °C
y = 1.628x - 15.17
R² = 0.817
Air Temperature in °C
b1
Surface Temperature °C
y = 1.606x - 18.60
R² = 0.955
Air Temperature in°C
c1
Surface Temperature °C
y = 1.298x - 9.880
R² = 0.932
Air Temperature in°C
d1
Surface Temperature °C
y = 1.538x - 15.01
R² = 0.970
Air Temperature in°C
e1
Surface Temperature in °C
y = -0.307x + 51.26
R² = 0.293
Relative Humidity in %
f1
Surface Temperature °C
y = -0.084x + 35.79
R² = 0.027
Relative Humidity in%
g1
Surface Temperature °C
y = 0.044x + 20.95
R² = 0.010
Relative Humidity in %
h1
Surface Temperature °C
y = -0.110x + 36.34
R² = 0.051
Relative Humidity in %

Table 5 Statistical analysis for different surfaces with Air temperature and relative humidity, Dibrugarh, 2019

Surface type	Time	(Air temperature)				(Relative humidity)			
		R	r^2	Coefficient of Determination (in %)	P value	R	r^2	Coefficient of Determination (in %)	P value
Asphalt	11.30 am	0.91	0.84	84	0.00004	−0.45	0.20	20	0.14
	3.30 pm	0.95	0.90	90	0.00006	−0.12	0.01	1	0.7
	6.30 pm	0.98	0.95	95	0.00001	−0.02	0.00	0	0.9
Grass	11.30 am	0.89	0.80	80	0.0017	−0.48	0.23	23	0.11
	3.30 pm	0.72	0.53	53	0.07	0.13	0.02	2	0.68
	6.30 pm	0.92	0.84	84	0.0006	0.20	0.04	4	0.53
Bare soil	11.30 am	0.90	0.82	82	0.001	−0.49	0.24	24	0.10
	3.30 pm	0.96	0.91	91	0.00004	−0.25	0.06	6	0.43
	6.30 pm	0.94	0.89	89	0.0001	0.13	0.02	2	0.68

than the surrounding natural rural environment. In general, different materials have different emission capacity. With these important heat-absorbing materials, combined with the heat generated from vehicles, air conditioners and industries enhances cities to generate, absorb and hold heat effectively. As a result, the heat captured during the day by diverse surfaces is gradually released at night (Lo and Quattrochi 2003; Solecki et al. 2005). Among all the surfaces, asphalt surface denoted maximum surface temperature and on the whole a dominating role in the development of surface urban heat island process. Low wind speed with higher air temperature and a lesser amount of humidity conditions added with anthropogenic process speed up the phenomenon of SUHII (surface urban heat island intensity). However, plantation of vegetation/trees along the urban streets as well as alongside the centerline of the major streets may act as a supporting function in providing shade, cooling effect as well as in lessening of the surface temperature of asphalt pavement and extenuating overall surface urban heat island effect of a city. The present study provides essential knowledge to help urban designers mitigate the SUHII. In the future, more in situ data will provide a more detailed thermal scenario of the city for strategic urban planning and for modeling studies to estimate the effect of the different measures.

As mentioned earlier, green spaces could improve the thermal discomfort during the period of heat stress (Lafortezza et al. 2009), increasing the percentage of vegetation areas and adopting light-colored building are the mitigation strategies to reduce the heat stress (Hoverter 2012). Finally, this study would give a novel methodological setup to comprehend the spatiotemporal nature of SUHII phenomena.

Acknowledgement The authors acknowledge the anonymous reviewers for their valuable inputs toward the improvement in this research article.

Compliance with ethical standards

Conflict of interest The authors of the manuscript declare no conflict of interest.

References

Akbari H, Konopacki SJ (1998) The impact of reflectivity and emissivity of roofs on building cooling and heating energy use. In: Proceedings of the thermal performance of the exterior envelopes of building VII, 6–10 December, pp 6–10

Almusaed A (2011) The urban heat island phenomenon upon urban components. In: Biophilic and bioclimatic architecture. Springer, London, pp 139–150

Becker F, Li Z-L (1993) Surface temperature and emissivity at various scales: definition, measurement and related problems. Remote Sens Rev 12:25–253

Becker F, Li ZL (1995) Surface temperature and emissivity at various scales: definition, measurement and related problems. Remote Sens Rev 12(3–4):225–253. https://doi.org/10.1080/02757259509532286

Census of India (2011) Office of the Registrar General & Census Commissioner, New Delhi

Chandler TJ (1965) The climate of London. Hutchinson, London

Choi Y-Y, Myoung S-S, Park K-H (2014) Assessment of surface urban heat Islands over three megacities in East Asia using LST data retrieved from COMS. Remote Sens. 6:5852–5867. https://doi.org/10.3390/rs6065852

Georgakis C, Santamouris M (2017) Determination of the surface and canopy urban heat Island in Athens central zone using advanced monitoring. Climate 5:97. https://doi.org/10.3390/cli5040097

Guhathakurta S, Gober P (2007) the impact of the Phoenix urban heat island on residential water use. J Am Plan Assoc 73:317–329

Hoverter SP (2012) Adapting to urban heat: a tool kit for local governments. Georgetown Climate Center, Washington, DC

Hu Y, Gensuo J (2010) Influence of land use change on urban heat island derived from multi-sensor data. Int J Climatol 30:1382–1395

Kumar KS, Bhaskar PU, Kumari KP (2017) Assessment and mapping of urban heat Island using field data in the new capital region of Andhra Pradesh. Indian J Sci Technol, India. https://doi.org/10.17485/ijst/2017/v10i11/99983

Lafortezza R, Carrus G, Sanesi G, Davies C (2009) Benefits and well-being perceived by people visiting green spaces in periods of heat stress. Urban For Urban Green 8:97–108

Liu L, Zhang Y (2011) Urban heat island analysis using the landsat TM data and ASTER data: a case study in Hong Kong. Remote Sens 3:1535–1552

Lo C, Quattrochi DA (2003) Land-use and land-cover change, urban heat island phenomenon, and health implications. Photogramm Eng Remote Sens 69:1053–1063

Neog R, Acharjee S, Hazarika J (2019) Evaluation of spatio-temporal pattern of surface urban heat island phenomena at Jorhat, India. Arab J Geosci 12:316. https://doi.org/10.1007/s12517-019-4484-z

Oke TR (1973) City size and the urban heat island. Atmos Environ 7(769–779):2

Oke TR (1982) the energetic basis of the urban heat Island. Q J R Meteorol Soc 108:1–24

Rasul A, Balzter H, Smith C, Remedios J, Adamu B, Sobrino J, Srivanit M, Weng Q (2017) A review on remote sensing of urban heat and cool islands. Land 6(2):38

Roth M, Oke TR, Emery WJ (1989) Satellite derived urban heat islands from three coastal cities and the utilization of such data in urban climatology. Int J Remote Sens 10:1699–1720

Shamsipour AA, Azizi G, Ahmadabad MK, Moghbel M (2013) Surface temperature pattern of asphalt, soil and grass in different weather condition. J Biodivers Environ Sci 3(9):80–89

Sharifi E, Soltani A (2017) Patterns of urban heat island effect in adelaide: a mobile traverse experiment. Mod Appl Sci. https://doi.org/10.5539/mas.v11n4p80

Solecki WD, Rosenzweig C, Parshall L, Pope G, Clark M, Cox J, Wiencke M (2005) Mitigation of the heat island effect in urban New Jersey. Glob Environ Change Part B Environ Hazards 6:39–49

Unger J, Sümeghy Z, Zoboki J (2001) Temperature cross-section features in an urban area. Atmos Res 58(2):117–127

Sundborg Å (1950) Local climatological studies of the temperature conditions in an urban area. Tellus 2(3):222–232

Voogt JA (2004) Urban heat island: hotter cities; action bioscience: North Port, FL, USA. http://www.actionbioscience.org/environment/voogt.html

Voogt JA, Oke TR (2003) Thermal remote sensing of urban climates. Remote Sens Environ 86:370–384

Yao R, Wang L, Huang X, Gong W, Xia X (2019) Greening in rural areas increases the surface urban heat Island intensity. Geophys Res Lett 46(4):2204–2212

Yilmaz H, Toy S, Irmak MA, Yilmaz S, Bulut Y (2008) Determination of temperature differences between asphalt concrete, soil and grass surfaces of the City of Erzurum. Turk Atmós 21(2):135–146

Publisher's Note Springer Nature remains neutral with regard to jurisdictional claims in published maps and institutional affiliations.